www.lajss.org
Latin American Journal of Solids and Structures 3 (2006) 197–222

Structural reliability analysis using deterministic finite element programs

André T. Beck*,[1] and Edison da Rosa[2]

[1]Engenharia de Estruturas, Escola de Engenharia de São Carlos, Universidade de São Paulo, SP – Brazil
[2]Departamento de Engenharia Mecânica, Universidade Federal de Santa Catarina, SC – Brazil

Abstract

The paper shows how structural reliability algorithms can be incorporated into deterministic (commercial) finite element codes and used to perform numerical structural reliability analysis based on finite element models of a structure. A structural reliability module is developed and linked to the ANSYS finite element program, creating a customized version of the program. Structural reliability analysis can be performed in the ANSYS environment, and involves construction of a parametric finite element model, definition of random parameter distributions, definition of a limit state function based on finite element results, and solution for the failure probability. Numerical examples involving truss and frame structures are studied. An application example - structural reliability analysis of an eye-bar suspension bridge - is also presented.

1 Introduction

In the last decades, numerical solutions to engineering problems have been widely developed. The versatility, broadness and accuracy of numerical (e.g. finite element) solutions have reached wide acceptability by the engineering practice.

The finite element solution, however, is only a solution to the mathematical model of the underlying engineering problem. Solution of the actual problem involves, in addition, a physical (behavioral) model, a failure model, selection of characteristic values for problems parameters and selection of suitable safety coefficients.

The need for safety coefficients is also widely accepted as due to the various sources of uncertainty which affect engineering problems. These uncertainties include natural randomness of problem parameters like material resistance and environmental loads, modelling uncertainty (the discrepancy between the result of failure models and results of failure tests), statistical uncertainty, decision uncertainty, human error and phenomenological uncertainty [11].

Structural reliability theory allows some of these uncertainties to be quantified and included explicitly in the analysis. In consideration of these uncertainties, structural reliability analysis

*Corresp. author email: atbeck@sc.usp.br Received 29 Sep. 2005; In revised form 3 May 2006

yields a quantifiable measure of structural safety, the failure probability, as shown in schematic form in Figure 1. Structural reliability methods can be used to guide the choice of characteristic values and safety coefficients to be used in a given project. This is particularly important in the design of novel structures for which design standards do not apply, in the design of unique structures and in the re-habilitation analysis of existing structures which have overcome their original design lives.

On the other hand, structural reliability methods are of little use if they cannot be used in conjunction with the best available techniques for solving the mechanical part of the problem. This includes a proper mechanical (behavioral) model of the problem and an accurate solution scheme for the mathematical model. Hence, it becomes very important to couple structural reliability algorithms with finite element analysis of structural problems.

This paper lays out the basis at which such coupling can be performed. It shows how structural reliability algorithms can be incorporated into deterministic finite element programs. The paper shows the implementation of a structural reliability module for the ANSYS program, and presents the analysis of some truss and frame structures. An application example involving an eye-bar suspension bridge is also presented.

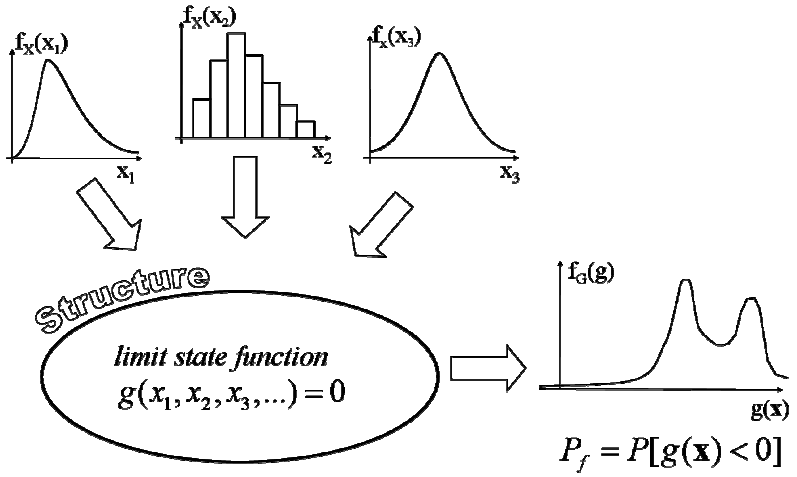

Figure 1: Reliability analysis of a structure with random parameters.

2 Coupling of reliability and structural analysis

Consider a structural problem where random or uncertain parameters are characterized in terms of random variables x_i (Figure 1). Each random variable is characterized by a marginal probability density function $f_{X_i}(x_i)$ and its parameters. Random variables may include material properties, geometric variables or loads. The vector of random problem parameters is denoted

by $\mathbf{X}$ and the correlation between pairs of random variables is represented by a correlation matrix $\mathbf{C}$, whose therms ρ_{ij} are the correlation coefficients between variables i and j.

Loading of the structure produces a set of load effects $\mathbf{s}(\mathbf{x})$, which include deformations, stresses and deflections. For a given failure mode (e.g. excessive deflection, yielding, instability), a limit state function is written in terms of load effects and some critical value x_c (e.g. ultimate stress, admissible deflection):

$$g(\mathbf{s}(\mathbf{x}),x_c) = \mathbf{0} \tag{1}$$

Critical effect x_c can be random or deterministic. The limit state equation is explicit in terms of load effects $\mathbf{s}(\mathbf{x})$, but contains the vector of problem parameters $\mathbf{x}$ implicitly. It is important to note that the relation between problem parameters $\mathbf{x}$ and load effects $\mathbf{s}(\mathbf{x})$ is given by the numerical (finite element) solution of the problem.

The limit state function is defined in such a manner that it divides the failure (D_f) and survival (D_s) domains:

$$\begin{aligned} D_f &= \{\mathbf{x}|g(\mathbf{x},x_c) \leq 0\} \\ D_s &= \{\mathbf{x}|g(\mathbf{x},x_c) > 0\} \end{aligned} \tag{2}$$

Failure probability with respect to a given failure mode is given by the integral of the joint probability density function over the failure domain:

$$P_f = \int_{g(\mathbf{x},x_c)\leq\mathbf{0}} f_{\mathbf{X}}(\mathbf{x})d\mathbf{x} \tag{3}$$

where $f_{\mathbf{X}}(\mathbf{x})$ is the joint probability density function (PDF) of the problems random variables. The integrand $f_{\mathbf{X}}(\mathbf{x})$ is usually approximated by marginal densities $f_{X_i}(x_i)$ and the correlation coefficients ρ_{ij}.

The integration domain in equation (3) is not known in closed form, but is given numerically as the solution to the finite element model. For each realization $\mathbf{X} = \mathbf{x}$ of the vector of random variables, a (deterministic) solution of the finite element model yields a numerical value for the limit state equation. This allows equation (3) to be evaluated using the finite element model of the structure as a black-box, as shown in Figure 2. The structural reliability algorithm establishes the points where $g(\mathbf{x},x_c)$ is to be evaluated, and guides the solution for failure probabilities. This independence between the structural reliability module and the finite element solution makes the integration with commercial (deterministic) finite element programs possible.

Using crude Monte Carlo Simulation, equation (3) is solved directly, by sampling the problems random variables following the density $f_{\mathbf{X}}(\mathbf{x})$ and evaluating the limit state function for each sampled point. This requires repetitive solutions of the finite element model, and is very costly in computation time if the failure probability is small.

More efficient solutions can be employed. In the First- and Second-Order Reliability Methods (FORM and SORM), integral (3) is solved in a transformed space of Standard Gaussian variables,

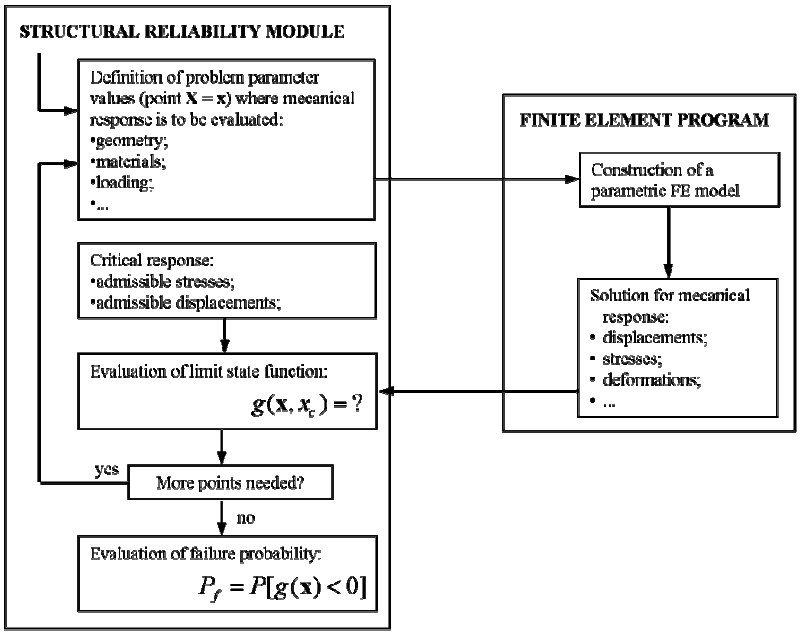

Figure 2: Independence between structural reliability module and finite element solution in structural reliability analysis.

and the integration boundary is approximated by an hyper-plane (FORM) or second-order surface (SORM). A more efficient sampling scheme (importance sampling) can be constructed using information obtained from a FORM analysis. These schemes will be presented in the sequence.

3 Structural reliability fundamentals

3.1 FORM - First order reliability method

In the FORM (and SORM) solutions, the original set of (possibly correlated) random variables $\mathbf{x}$ is transformed into a set of uncorrelated standard Gaussian variables $\mathbf{y}$ by the transformation:

$$\mathbf{y} = \mathbb{T}(\mathbf{x}) \tag{4}$$

This transformation involves:

1. an evaluation of Gaussian distributions that are equivalent to the original marginal densities $f_X(x)$ and;
2. elimination of the correlation between original variables.

This transformation allows equation (3) to be solved approximately by making use of the symmetry of the (uncorrelated) joint standard Gaussian distribution $f_{\mathbf{Y}}(\mathbf{y})$. If $\mathbf{J}$ is the Jacobian of the transformation from $\mathbf{x}$ to $\mathbf{y}$, the desired transformation is:

$$\mathbf{y} = \mathbf{J} \cdot \{\mathbf{x} - \mathbf{M}^{neq}\} \tag{5}$$

In equation (5), the Jacobian is evaluated as:

$$\mathbf{J} = \mathbf{L}^{-1} \cdot (\mathbf{D}^{neq})^{-1} \tag{6}$$

and:
$\mathbf{M}^{neq}$ is the vector of means of the equivalent normal distributions;
$\mathbf{D}^{neq}$ is the diagonal matrix whose elements are the standard deviations of the equivalent normal distributions and
$\mathbf{L}^{-1}$ is the lower triangular matrix obtained by Choleski decomposition of correlation matrix $\mathbf{C}$.

Parameters (means and standard deviations) of the equivalent Gaussian distributions are obtained using the Principle of Normal Tail Approximation [7]. This yields:

$$\begin{aligned} \sigma_{X_i}^{neq} &= \frac{\phi\left(y_i^*\right)}{f_{X_i}(x_i)} \\ \mu_{X_i}^{neq} &= x_i^* - y_i^* \cdot \sigma_{X_i}^{neq} \end{aligned} \tag{7}$$

where $\phi(.)$ is the standard Gaussian density and $y_i^* = \Phi^{-1}(F_{X_i}(x_i^*))$ is the point in standard Gaussian space where the transformation is being made. The transformation also involves the evaluation of equivalent correlation coefficients [8].

With the transformation to the standard Gaussian space, the rotational symmetry of the joint density $f_{\mathbf{Y}}(\mathbf{y})$ is used to approximate the integral in equation (3). As shown in Figure 4, the point over the limit state surface which is closest to the origin of the standard Gaussian space is also the point over the failure domain with the greatest probability of occurrence. Therefore, this is also an appropriate point to approximate the original limit state function $g(\mathbf{x},x_c)$ by an hyper-plane (the first order approximation). This point is also known as the *design point*, and it corresponds to that realization (among all possible) of the problems random variables which is more likely to cause failure of the structure. The (minimal) distance between the design point and the origin is called reliability index (β). The first order approximation to the failure probability is:

$$P_{f_1} = \Phi(-\beta) \tag{8}$$

where $\Phi(.)$ is the cumulative standard Gaussian distribution.

Because of this minimum property, the design point and reliability index β are found (numerically) using a convenient optimization scheme. The optimization problem is stated as:

$$\begin{aligned} &\text{minimize: } d^2 = \mathbf{y}^T \cdot \mathbf{y} \\ &\text{subject to: } g(\mathbf{y}) = 0 \end{aligned} \tag{9}$$

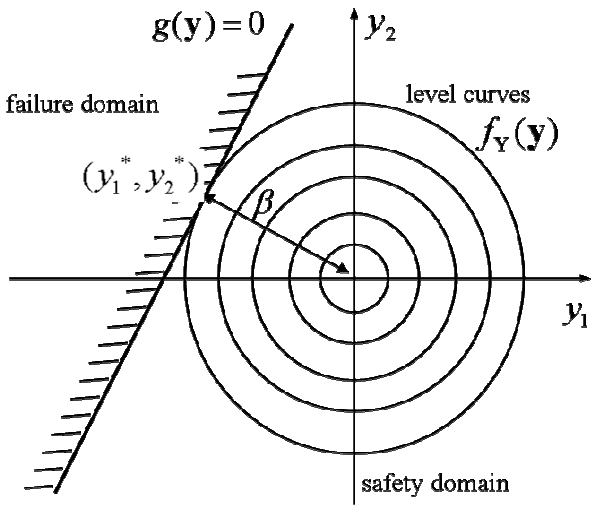

Figure 3: First-order approximation in standard normal space.

The minimum is β^2 and the minimum point is the design point $\mathbf{y}^*$. The very simple HLRF algorithm [12, 13] can be used to solve the optimization problem. Starting from a point $\mathbf{y}_k$, the next point in the iteration is:

$$\mathbf{y}_{k+1} = \frac{\nabla g(\mathbf{y}_k)^T \cdot \mathbf{y}_k - g(\mathbf{y}_k)}{\nabla g(\mathbf{y}_k)^T \cdot \nabla g(\mathbf{y}_k)} \cdot \nabla g(\mathbf{y}_k) \tag{10}$$

where $\nabla g(\mathbf{y}_k)$ is the gradient of the limit state surface with respect to the random variables, calculated in the standard Gaussian space.

The gradient can be evaluated in original $\mathbb{X}$ space by finite difference or by means of Direct Differentiation [9]. Direct Differentiation involves an analytical derivation of finite element equilibrium equations in terms of response quantities. It yields a set of (finite element) equations to be solved for terms of the gradient of response quantities. The contribution of gradient terms is assembled in a global gradient stiffness matrix, which is solved for the desired gradients. The gradient evaluated in $\mathbb{X}$ space is transformed into $\mathbb{Y}$ space using the transformation:

$$\nabla g(\mathbf{y}) = (\mathbf{J}^{-1})^T \cdot \nabla g(\mathbf{x}) \tag{11}$$

In this paper, a finite difference scheme is used to compute the gradients. This avoids programming of finite element routines and allows the finite element code to be used without alteration.

3.2 SORM - Second order reliability method

First order estimates of the failure probability can be improved by taking into account the curvatures of the limit state surface at the design point. In the Second Order Reliability Method

(SORM), a second-order surface is used to approximate the limit state function at the design point. When an hyper-paraboloid is fitted so that its principal curvatures coincide with the principal curvatures (k_i) of the limit state surface, the SORM estimate of the failure probability becomes [6]:

$$P_{f_2} = \Phi(-\beta) \prod_{i=1}^{n_{rv}-1} \frac{1}{\sqrt{1-\beta k_i}} \tag{12}$$

where n_{rv} is the number of random variables.

3.3 Multiple failure modes

Structural members can usually fail in a multitude of manners. Each failure mode gives rise to one limit state function. Failure of the member is characterized by failure in any of the possible failure modes, i.e. the limit state functions for a structural member are associated as a series system.

In the case of isostatic structures (structures with little redundancy), failure of any of its members causes failure of the structure. For hyperstatic structures with multiple member redundancy, progressive failure of members has to be considered.

The failure probability of members with multiple failure modes (series system) cannot be obtained in closed form, unless some simplifications are considered. Bounds for the failure probability of the member can be derived from individual failure probabilities by linearizing each limit state functions at its design point. Considering joint failure in two modes and neglecting triple failure mode combinations, one obtains the bimodal bounds [1]:

$$P[F_1] + \sum_{i=2}^{n_{fm}} \max \left[P[F_i] - \sum_{j=1}^{i-1} \left(P(A_{ij}) + P(B_{ij}) \right); 0 \right] \leqslant P_f$$

$$P_f \leqslant \sum_{i=1}^{n_{fm}} P[F_i] - \sum_{i=2}^{n_{fm}} \max_{i>j} \left[\max[\, P(A_{ij}), P(B_{ij})] \right] \tag{13}$$

where n_{fm} is the number of failure modes and where individual failure modes (F_i) are arranged in decreasing order of failure probability.

The linearized correlation coefficient between two failure modes is evaluated at the respective design points as:

$$\rho_{ij} = \frac{\nabla g_i \cdot \nabla g_j}{|\nabla g_i| \cdot |\nabla g_j|} \tag{14}$$

The probabilities $P(A_{ij})$ and $P(B_{ij})$ in equation (13) are calculated as:

$$P(A_{ij}) = \Phi(-\beta_i) \cdot \Phi\left(-\frac{\beta_j - \rho_{ij} \cdot \beta_i}{\sqrt{1-\rho_{ij}^2}}\right)$$
$$P(B_{ij}) = \Phi(-\beta_j) \cdot \Phi\left(-\frac{\beta_i - \rho_{ij} \cdot \beta_j}{\sqrt{1-\rho_{ij}^2}}\right) \tag{15}$$

When two or more failure modes are equivalent, the bounds given in equation (13) can be quite large. The bounds are asymptotic, i.e., they get narrower as the failure probability decreases. Results for multiple failure modes can be improved with importance sampling, as will be seen later.

3.4 Response surface

The reliability analysis based on a numerical (finite element) model of a structure can also be performed by means of a response surface. An approximate polynomial model of the structure (the response surface) can be constructed by curve fitting to a set of points evaluated from the numerical model of the problem. The polynomial model is then used for the reliability computation (e.g. Monte Carlo simulation) with a great speed-up in computation time. A second-order response surface is obtained as:

$$g_{rs}(\mathbf{x}) \approx a + \mathbf{x} \cdot \mathbf{b} + \mathbf{x}^T \cdot \mathbf{c} \cdot \mathbf{x} \tag{16}$$

where $a, \mathbf{b}, \mathbf{c}$ contain the coefficients to be determined. Construction of a complete second-order surface requires the evaluation of the limit state at $(1 + n_{rv} + n_{rv}^2)$ points, where n_{rv} is the number of random variables. A cruder version, without cross terms, can also be used. In this case, only $(2n_{rv} + 1)$ points have to be evaluated. In this paper, vector $\mathbf{b}$ and matrix $\mathbf{c}$ are approximated by the gradient and the Hessian of the limit state surface, which are computed by central differences. The required number of limit state evaluations is $(2n_{rv}^2)$ for each response surface.

One significant improvement over a "crude" response surface analysis is to construct response surfaces around the design points. This ensures that curve fitting is performed around the most important failure regions, and errors of approximating the numerical response by analytical surfaces are reduced. In this case, design points are first found using the HLRF algorithm.

3.5 Monte Carlo simulation

3.5.1 Simple sampling

In simple (crude) Monte Carlo simulation, samples of $\mathbf{x}$ are generated according to the original joint probability density function $f_{\mathbf{X}}(\mathbf{x})$. Using and indicator function $I_{[g(\mathbf{x})]}$, integration for the failure probability in equation (3) is extended over the whole domain:

$$P_f = \int_{\text{all } \mathbf{x}} I_{[g(\mathbf{x})]} f_{\mathbf{X}}(\mathbf{x}) d\mathbf{x} \tag{17}$$

The state of the structure (either failure or survival) for each sample point is given by the indicator function:

$$\begin{aligned} I_{[g(\mathbf{x}_i)]} &= 1 \text{ if } g(\mathbf{x}_i) \leq 0 \\ I_{[g(\mathbf{x}_i)]} &= 0 \text{ if } g(\mathbf{x}_i) > 0 \end{aligned} \tag{18}$$

The failure probability is estimated from eq. (17) as:

$$\overline{P_f} = \frac{\sum_{i=1}^{n_{si}} I_{[g(\mathbf{x}_i)]}}{n_{si}} \tag{19}$$

Simulation results are subject to a statistical sampling error. Variance of the estimated failure probability is:

$$Var_{(\overline{P_f})} = \frac{\sum_{i=1}^{n_{si}} \left(I_{[g(\mathbf{x}_i)]} - \overline{P}_f \right)^2}{n_{si}(n_{si} - 1)} \tag{20}$$

Due to the small failure probability of engineering structures, usually a very large number of samples is required in crude Monte Carlo in order to keep the variance within acceptable limits. Variance of results can be reduced by increasing the number of samples or by making use of importance sampling, which shifts sampled points to more important regions of the failure domain.

3.5.2 Importance sampling

With importance sampling, a sampling function $h_{\mathbf{X}}(\mathbf{x})$ is used to generated the samples. Each sampled point $\mathbf{x}_i$ is associated to a sampling weight $w_i = f_{\mathbf{X}}(\mathbf{x}_i)/h_{\mathbf{X}}(\mathbf{x}_i)$, and the failure probability is given by:

$$\overline{P_f} = \frac{1}{n_{si}} \sum_{i=1}^{n_{si}} I_{[g(\mathbf{x}_i)]} \frac{f_{\mathbf{X}}(\mathbf{x}_i)}{h_{\mathbf{X}}(\mathbf{x}_i)} \tag{21}$$

A very efficient sampling scheme is *importance sampling using design points* [5]. This technique makes intelligent use of a priory knowledge: location of the most important failure regions, around the design points.

The sampling function $h_{\mathbf{X}}(\mathbf{x})$ for multiple failure modes is constructed following [14]. The design points are first found using the HLRF algorithm. The FORM estimate of individual failure probabilities shows the relative importance of each design point. Simulation weights p_j are calculated based on FORM results:

$$p_j = \frac{\Phi(-\beta_j)}{\sum_{j=1}^{k} \Phi(-\beta_j)}$$

The sampling function is constructed as to have one bulge over each design point and to be flat elsewhere, as shown in Figure 5. Each bulge $h_{j\mathbf{X}}$ is obtained by shifting the original joint PDF to the respective design point. The bulges are scaled according to sampling weight p_j, and the sampling function results:

$$h_{\mathbf{X}}(\mathbf{x}) = \sum_{j=1}^{k} p_j h_{j\mathbf{X}}(\mathbf{x})$$

When importance sampling (using design points) is used, the required number of samples is virtually independent of the order of magnitude of the failure probability. Usually, 2000 to 3000 sample points will be required for a 5-10% variance.

The importance sampling simulation can be performed using the finite element model directly or using the response surfaces fitted to each design point. When the number of random variables and limit state functions is not large, it is convenient to use response surfaces. Using response surfaces as proposed in this paper is convenient when ($2n_{rv}^2 n_{fm} < 3000$), where n_{fm} is the number of failure modes.

The importance sampling scheme is particularly interesting for multiple failure modes. For each sampled point, all limit state functions are checked. The failure probability for individual failure modes and for any combination of series and parallel failure modes is easily computed. Simulation using second-order response surfaces is a significant improvement over linearized bimodal bounds (eq. 13).

3.6 Sub-modelling

Structural reliability algorithms, when coupled with finite element models of a structure, can be used to evaluate failure probabilities or to obtain the probability density distribution of response quantities (load effects). When using sub-models in the structural (finite element) analysis, response probability densities are necessary in order to construct the (sub-model) reliability problem.

The distribution of displacements or stresses acting on the sub-model can be determined from the distribution of original random variables by repeatedly solving the structural reliability problem of the global finite element model. This is done by varying the critical variable s_c for a given response quantity $s(\mathbf{x})$ over its whole range. The cumulative distribution of S is obtained as:

$$\begin{aligned} F_S(s_c) &= P[S < s_c] \\ &= \int_{g(\mathbf{x},s_c)\leq 0} f_{\mathbf{X}}(\mathbf{x}) d\mathbf{x} \end{aligned} \tag{22}$$

using the limit state function:

$$g(\mathbf{x},s_c) = S(\mathbf{x}) - s_c = 0 \tag{23}$$

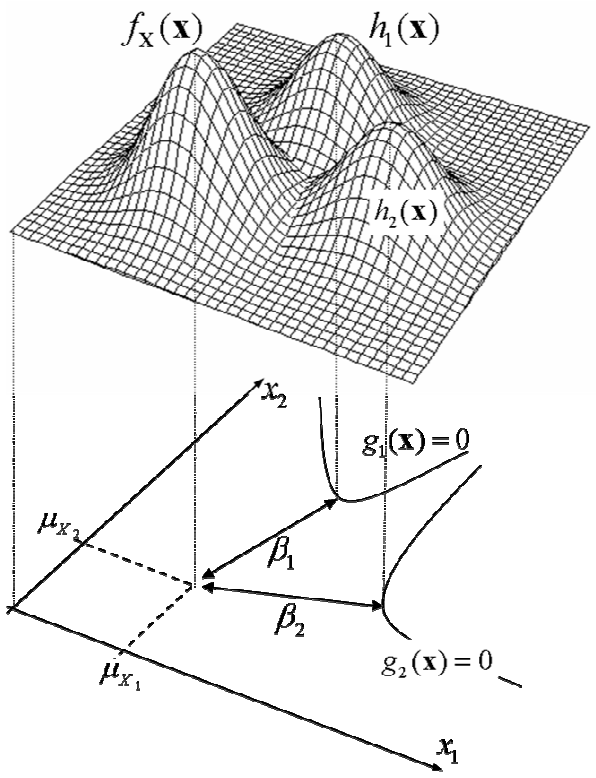

Figure 4: Importance sampling using design points.

The failure probability is then evaluated using the response quantity probability distribution and the finite element sub-model. Examples are shown in the sequel to illustrate this feature.

4 A structural reliability module for the ANSYS program

Structural reliability algorithms just described were programmed in Fortran, using the Digital Fortran 95 compiler. A structural reliability module was developed and linked to the ANSYS finite element program, creating a customized version of the program. The *User Programmable Feature* for optimization (file userop.f) was used to link the structural reliability module with ANSYS [2, 4].

The developed structural reliability module is depicted in Figure 5. The figure shows the modules main subroutines. The finite element program is acessed by means of the *limit state evaluation* subroutine, as indicated in the figure. For each limit state function, the developed module:

1. finds the design point;

2. evaluates the first-order failure probability;

3. constructs a response surface centered at the design point;

When more than one failure mode exists, the module:

1. evaluates bi-modal failure bounds and

2. performs Monte Carlo simulation with importance sampling, using the constructed response surfaces.

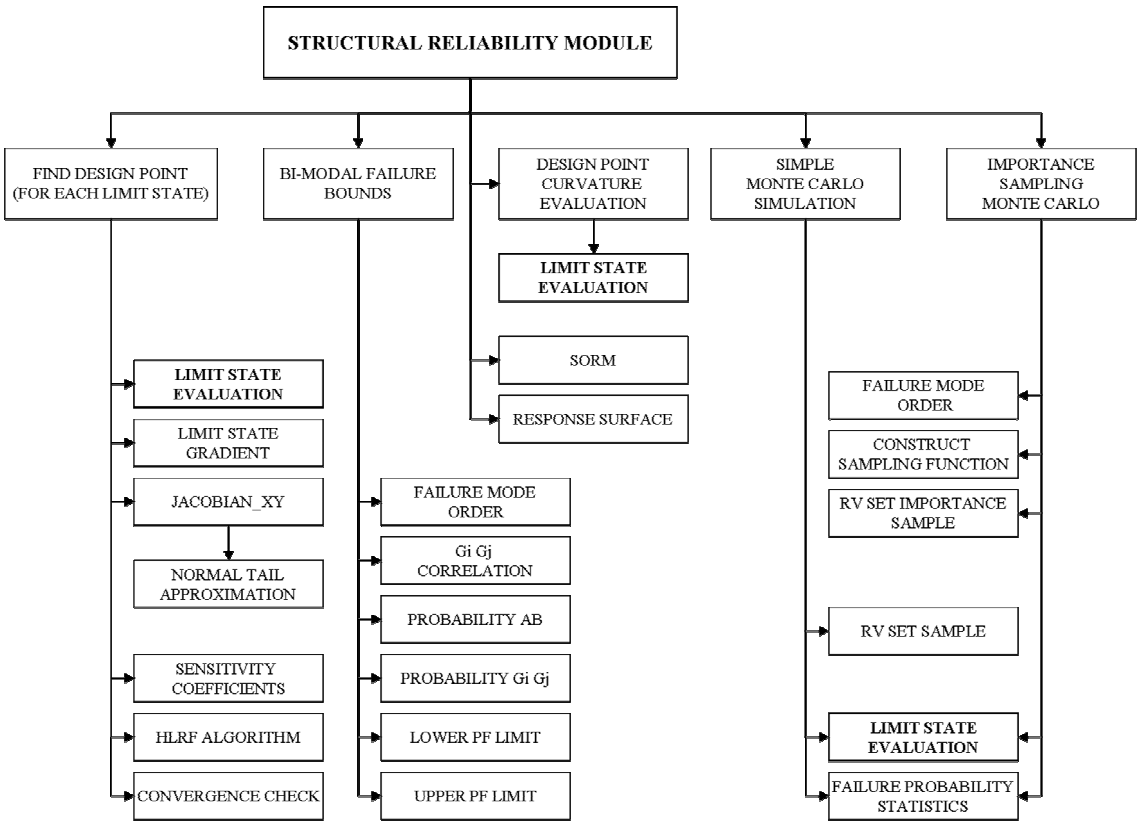

Figure 5: Fluxogram showing main routines of strutural reliability module.

A structural reliability analysis using ANSYS and the developed module is fully performed in the ANSYS program environment. It requires only two additional tasks, in comparison to a deterministic structural analysis:

1. construction of a parametric finite element model of the structure and;

2. statistical description of random problem parameters.

The parametric model is constructed similarly as in an ANSYS optimization analysis. The structural reliability module is accessed via the user optimization module. Each random variable and limit state function is defined as a parameter. The finite element model is constructed and the solution is obtained. Required load effects (stresses, displacements) are recovered from the solution and the limit state functions are defined. In the ANSYS optimization module, random variables are declared as design variables and limit state functions are declared as state variables. An objective function is defined only to fulfill ANSYS requirements. Results are written to a text file. Other details are given in ref. [3].

Some numerical examples follow.

5 Numerical examples

5.1 Cantilever beam

This example is taken from [10]. It is very simple on the mechanical point of view, but it has a highly non-linear limit state function. This allows an analysis of the accuracy of approximate solution methods. The limit state function corresponds to incipient yielding of the clamped end of the beam (elastic behavior):

$$g(\mathbf{x}) = S_y - \frac{3ql^2}{bh^2} = X_5 - \frac{3X_1X_2^2}{X_3X_4^2} = 0 \tag{24}$$

Data for this example is summarized in Table 1. Results for distinct solution methods are presented in Table 2.

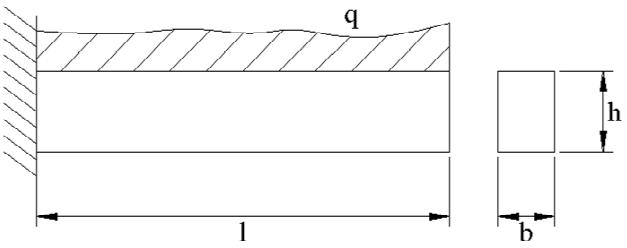

Figure 6: Cantilever beam.

Results agree with ref. [10]: $P_{f_1} = 0.100$ and $P_{f_2} = 0.103$, for FORM and SORM, respectively. Computation time for this example, using ANSYS, was only a few seconds, using a 80586, 300 MHz processor.

Failure probability for this example is large because the safety coefficient is small ($k = 1.16$). The solution was repeated by decreasing (in mean value) load variables q and l and by increasing

Table 1: Data for cantilever beam example.

RV		Distribution	μ	δ	Unit
X_1	q	Normal	1.15	0.029	kg/cm
X_2	l	Normal	60.00	0.010	cm
X_3	b	Normal	4.00	0.030	cm
X_4	h	Normal	1.00	0.030	cm
X_5	S_y	Normal	3600.00	0.083	kg/cm^2

Table 2: Results for the cantilever beam example.

Method	P_f	δ / toler.	n_{si} / n_{iter}
FORM	0.100	10^{-3}	5
SORM	0.104	10^{-3}	-
Crude MCS	0.103	0.009	10^5
Imp. Sampling	0.104	0.004	10^5
Crude MCS with Response Surface	0.107	0.009	10^5
Imp. Sampling with Response Surface	0.108	0.004	10^5

resistance variables (b, h and S_y), thus increasing the safety coefficient. Results are shown in Figure 7, in both linear and logarithmic scales. The figure shows the highly non-linear relation between safety factors and failure probabilities. It shows how structural reliability analysis can be used to guide selection of the safety factor. In this example, reducing the safety factor from 1.75 to 1.5 does not affect failure probability critically. But reducing the safety factor from 1.5 to 1.25 can be disastrous. On the other hand, it is seen that increasing the safety factor from 2.0 to 3.0 will only increase costs, with no important increase in reliability.

Figure 8 shows the sub-modelling feature for this problem. The probability density function for the maximum stress ($S_{\max} = 3ql^2/bh^2$) at the clamped end of the beam is obtained by making X_5 deterministic and varying its value. The resulting distribution is compared with that obtained by random variable algebra (Gaussian assumption). The figure shows that the high non-linearity of the limit state function does not significantly affect the maximum stress distribution, which is also closely Gaussian.

5.2 13 bar truss

This 13 bar truss example is taken from ref. [15]. Failure modes are yielding of each bar, resulting in 13 limit state functions. Yielding stress of each bar is assumed an independent random variable, with log-normal distribution. Load P is also a random variable.

The problem can be solved analytically by means of load factors, which relate the loading on each bar with applied load P. The limit state functions are:

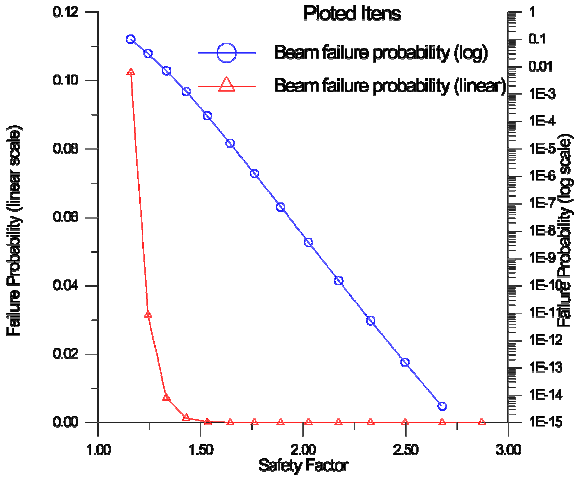

Figure 7: Relation between safety coefficient and failure probability.

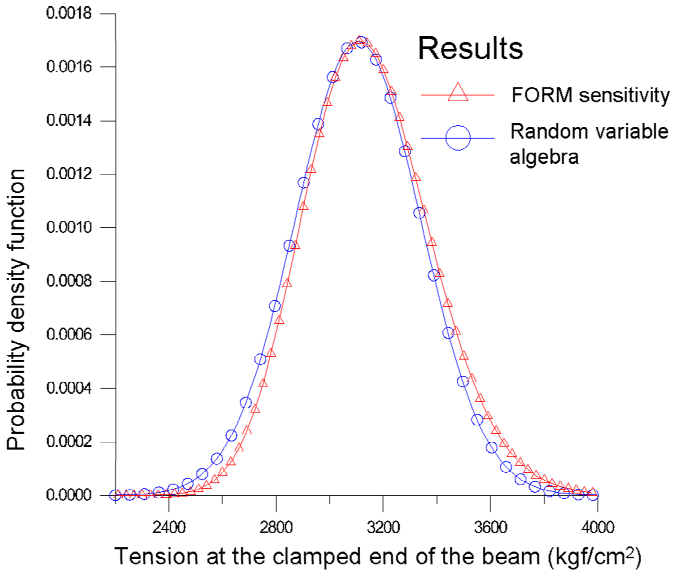

Figure 8: PDF of the maximum stress at the clamped end of the beam.

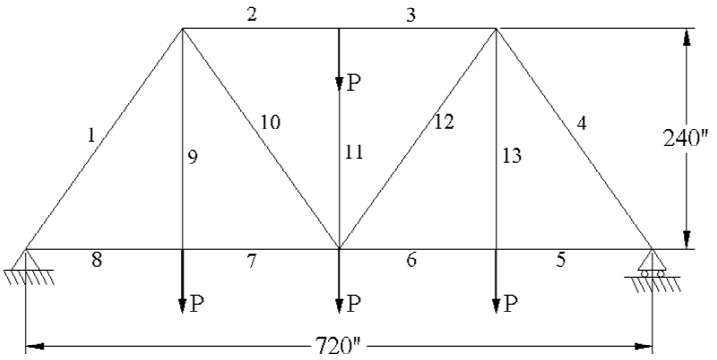

Figure 9: 13 bar truss example.

$$g_i(\mathbf{x}) = S_i A_i - a_i P = 0 \text{ for } i = 1, ..., 13$$

where:
S_i = yielding stress of the ith bar;
A_i = cross sectional area of the ith bar;
a_i = load factor for the ith bar.

Data for this example is presented in Tables 3 and 4. The results are presented in Table 5.

Table 3: Random variable data for 13 bar truss problem.

RV		Distribution	μ	δ	Unit
X_1	P	Log-normal	50250.63	0.10	lb
X_2 to X_{14}	S_i	Log-normal	40032.01	0.04	psi

Table 4: Data for deterministic parameters.

Bar	A_i (in^2)	a_i
1 and 4	4.80	2.50
2 and 3	4.80	2.25
5, 6, 7, and 8	2.10	1.50
9, 11 and 13	2.10	1.00
10 and 12	2.10	1.25

Results show that failure of the truss is mainly governed by bars 5 to 8. Results for the series system analysis agree with results in ref. [15], obtained with a convolution integral ($P_f = 0.2435$). Bimodal failure bounds for the series system analysis are very large in this example. This is due to the high correlation between the most important failure modes.

Table 5: Results for the 13 bar truss example (series system analysis).

Method	P_f	δ / toler.	n_{si} / n_{iter}
FORM - Bimodal limits	$0.1463 \leq P_f \leq 0.4154$	10^{-4}	5 per $g(\mathbf{x})$
Crude MCS	0.2434	0.008	5×10^4
Imp. Sampling	0.2447	0.004	5×10^4

Table 6: Results for individual bars.

Bars	P_f (FORM)
1 and 4	3.3×10^{-4}
2 and 3	3.5×10^{-7}
5, 6, 7 and 8	0.1463
9, 11 and 13	7.3×10^{-7}
10 and 12	3.0×10^{-3}

The safety coefficient for bar 5 is 1.12. Figure 10 shows the non-linear relation between safety factors and failure probabilities for the truss and for bar number 5.

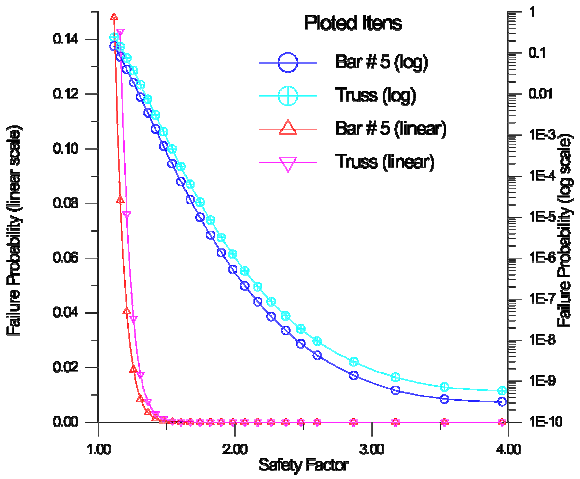

Figure 10: Relation between safety coefficient and failure probability.

Solution of this problem using a convolution integral [15] requires significant simplifications, like the assumption of independence between the yielding stresses and consideration of identical P loads. These simplifications would not be required in the present formulation. The developed structural reliability module allows solution of the problem in a more realistic basis.

5.3 Built-up column

This problem is taken from ref. [8]. Solution involves a non-linear finite element analysis, due to large deflections of the column. The failure mode considered is buckling. The problem involves 22 random variables: the elasticity modules of struts (E_1) and of braces and battens (E_2), two random forces F_1 and F_2 (following Figure 11) and 18 nodal coordinates. The vertical coordinate of each node is deterministic, but the horizontal coordinate is represented as a random variable. This takes into account the effect of geometric imperfections in the buckling load of the column.

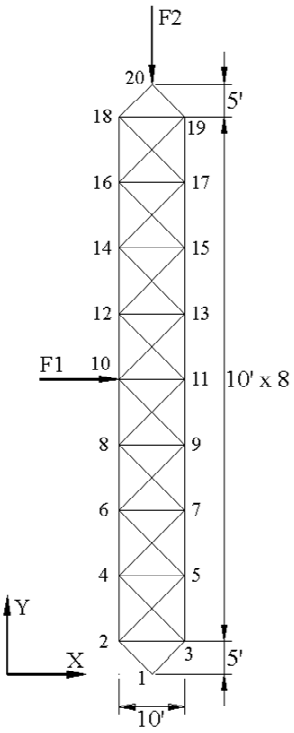

Figure 11: Built-Up column.

The limit state equation is written in terms of the horizontal displacement at the midspan of the column (node 10) and the critical displacement u_0:

$$g(\mathbf{x}) = u_0 - u_{10} = 0$$

Figure 12 shows the load-displacement curve for the column. From this figure, the critical displacement is set as $u_0 = 10$ inches. Data for this problem is summarized in Table 7.

The correlation coefficient between E_1 and E_2 is equal to 0.3. The remaining random variables are uncorrelated. Cross sectional areas of struts are 1.59 in^2 and of braces and battens are

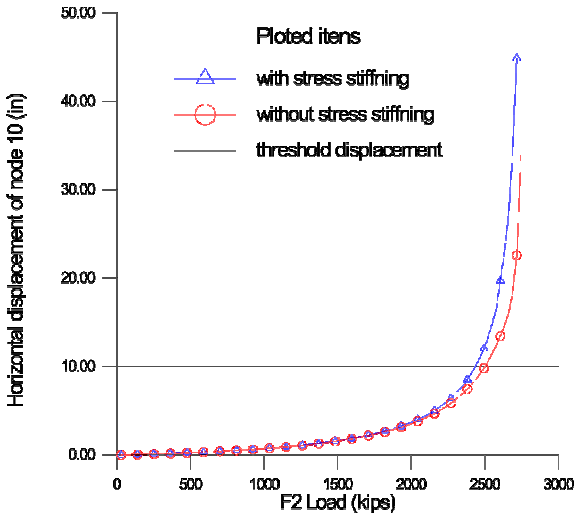

Figure 12: Load - displacement curve for the Built-Up column.

Table 7: Data for the built-up column problem.

RV		Distribution	μ	δ	Unit
X_1	E_1	Log-normal	30000.0	0.08	ksi
X_2	E_2	Log-normal	30000.0	0.08	ksi
X_3	F_1	Log-normal	20.0	0.10	kips
X_4	F_2	Log-normal	1500.0	0.10	kips
X_5 to X_{22}	x_2 to x_{18}	Normal	+60.0 or −60.0	0.02	in

Table 8: Results for the built-up column example.

Reference	Method	P_f	tolerance	n_{iter}
Liu and Kiureghian [10]	FORM	5.0×10^{-3}	?	8
Present analysis in ANSYS	FORM	1.1×10^{-4}	10^{-3}	8

0.938 in^2. Other dimensions are given in Figure 11. Failure probability results are presented in Table 8.

Results are in reasonable agreement, considering that the non-linear model used in the two studies was not exactly the same. Because each limit state evaluation requires a non-linear finite element analysis, the computation time increased reasonably for this problem. The FORM estimate was obtained in 2 minutes and construction of the response surface lasted 18 minutes. Much of this computation time is due to the finite difference scheme used in the gradient and Hessian computations.

For critical displacements larger that 10 inches ($u_0 > 10$) convergence problems were encountered. Therefore, a comparison between safety factor and failure probabilities was not possible. The safety factor for this example is 3.62.

Sensitivity coefficients of FORM solution are shown in Figure 13. Those coefficients show the relative importance of each random variable in failure of the column. Results show the relatively high importance of the uncertainty in the horizontal coordinate of the nodes, especially for those nodes situated at the midspan of the column. The figure also shows a large contribution of F_2, comparing to lateral load F_1. Uncertainty in elasticity modules affects reliability of the column more in struts than in braces and battens.

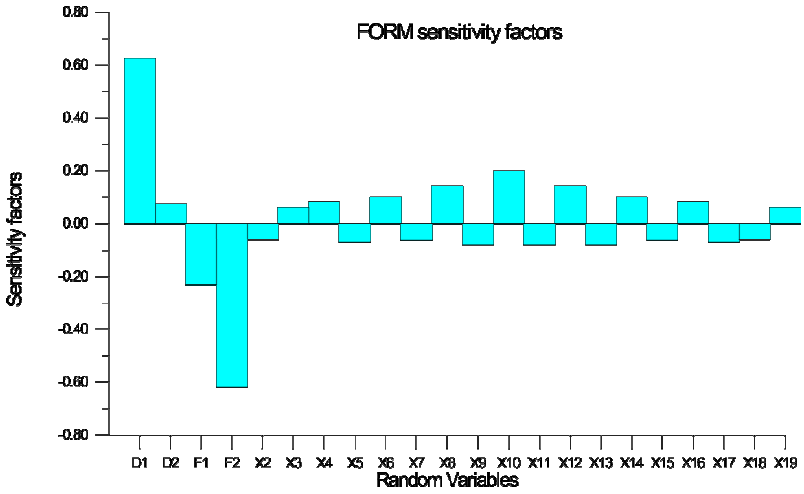

Figure 13: FORM sensitivity coefficients for the built-up column.

5.4 Application example: reliability analysis of an eye-bar suspension bridge

The developed structural reliability modules were employed in a simplified reliability analysis of an eye-bar suspension bridge (Hercílio Luz), located in the city of Florianópolis, Santa Catarina, Brazil, and built in 1926. The bridges suspension chain is composed of intercalated sets of four and five parallel eye bars connected by pins. A volume plot of part of the 3D finite element model used in the analysis is shown in Figure 14. The model has 2275 elements and 8886 degrees of freedom. Stress stiffening effects were considered in the analysis. Details of the eye-bar suspension chain are shown in Figure 15.

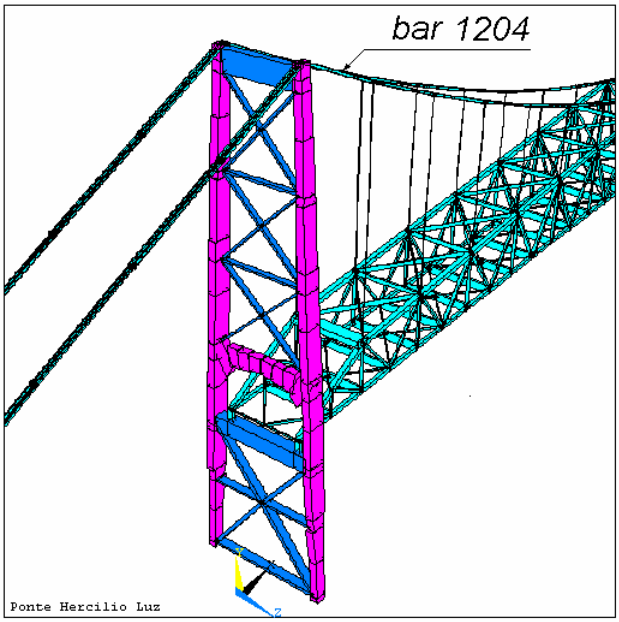

Figure 14: Volume plot of the bridges 3D finite element model.

In a simplified reliability analysis, only 5 random variables were considered: the distributed live load (q), yielding stress of the bars (S_y), the ultimate stress (S_u), the actual level of corrosion (area reduction) of the bars (γ) and the dead weight. The uncertainty in the dead weight was represented by means of an uncertainty in the gravity acceleration constant (g). Random variable data for the analysis is summarized in Table 9.

Several situations were analyzed in this study. In this paper, results for failure of an individual bar and for failure of the suspension chain are presented. The complete analysis is presented in Beck (1999). For failure of an individual bar, two limit states were considered:



Figure 15: Detailed view of suspension chain bars.

Table 9: Random variable data for bridge analysis.

Variable	Distribution	μ	δ	Unit
q	Gaussian	1.4×10^6	0.140	N
S_y	Weibull for minima	582.60	0.060	MPa
S_u	Weibull for minima	848.00	0.054	MPa
γ	Weibull for maxima	0.10	0.138	-
g	Gaussian	9.81	0.100	m/s^2

$$\begin{aligned} g_1(\mathbf{x}) &= S_y - S^{bar1204}_{membrane} \\ g_2(\mathbf{x}) &= S_u - S^{bar1204}_{membrane} \end{aligned} \tag{25}$$

Failure mode 1 represent yielding (plastification) of the whole section of a bar and failure mode 2 represent rupture of the bar. These limit states assume free rotation of the bar, hence only membrane stresses are included. Bar 1204 is the bar that fractured in use, but results are valid for any single bar of the suspension chain that is not part of the center frame.

Failure probability results are shown in Table 10:

Table 10: Results for the bridge analysis.

Failure mode	Safety factor	Failure Probability
yielding - $g_1(\mathbf{x})$	2.00	6.60×10^{-6}
rupture - $g_2(\mathbf{x})$	2.90	1.70×10^{-9}

Independent checking of these results was not possible, but they seem fairly reasonable. The computation time required in this case was 20 minutes for each limit state. Convergence of the solution in this study shows the developed structural reliability modules ability to handle large scale real world problems.

5.4.1 Failure of one module (4 bars)

Each module of the suspension chain is formed by 4 bars, connected to each other and to the next module by a pin. Failure of one individual bar does not necessarily cause failure of the suspension chain, as practice has shown (failure of bar 1204 with the bridge still standing). The four bars of a module form a parallel system with active redundancy.

Since failure of the 4 bars is not perfectly correlated, a conditional failure analysis has to be performed. For one module, there are $4! = 24$ possible failure sequences. The two most important failure sequences for one module are shown in Figure 16. Initial failure could be of any bar of the module.

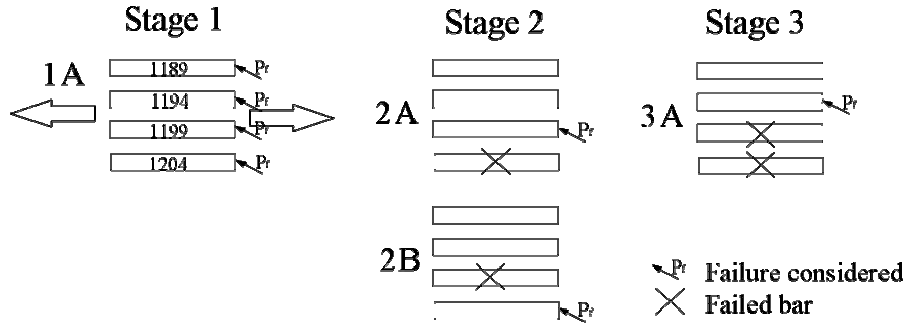

Figure 16: Most important failure sequences for one module.

The probability for the first bar failure is $P_f = 1.70 \times 10^{-9}$, corresponding to limit state function $g_2(\mathbf{x})$. In the second stage, the failure probability of the remaining bars given failure of the first bar is evaluated. For this analysis, a random impact factor with distribution $N(2, 0.5)$ was considered. Failure probability results and sensitivity coefficients for conditional failures are presented in Table 11.

The failure probability of the third bar, given failure of two bars (stage 3A), is fairly high. Hence, one can assume failure of the fourth bar, given failure of the third bar, as certain. Considering independence between bar failures, probability of occurrence of the two most important failure sequences (as shown in Figure 16) is:

$$\begin{aligned} P[\text{sequence 1}] &= 1.70 \times 10^{-9} \times 5.02 \times 10^{-4} \times 1.19 \times 10^{-2} = 1.01 \times 10^{-14} \\ P[\text{sequence 2}] &= 1.70 \times 10^{-9} \times 6.58 \times 10^{-5} \times 1.19 \times 10^{-2} = 1.33 \times 10^{-15} \end{aligned}$$

Table 11: Failure probability results and sensitivity coefficients for conditional failure of one module.

Stage	P_f	Sensit.				
		q	S_u	γ	g	impact factor
1A	1.70×10^{-9}	-0.22	0.95	-0.16	-0.13	–
2A	5.02×10^{-4}	-0.48	0.29	-0.42	-0.28	-0.65
2B	6.58×10^{-5}	-0.47	0.28	-0.52	-0.27	-0.59
3A	1.19×10^{-2}	-0.53	0.22	-0.36	-0.31	-0.66

Taking into account the symmetry of the module, both sequences can occur in two distinct forms. Considering failure sequences to be independent and mutually exclusive, the failure probability for a suspension chain module is:

$$P[\text{module failure}] = 2 \times P[\text{sequence 1}] + 2 \times P[\text{sequence 2}] = 2.86 \times 10^{-14}$$

Unimodal failure probability bounds for a suspension chain module are:

$$2.86 \times 10^{-14} \leq P[\text{module failure}] \leq 1.70 \times 10^{-9}$$

The lower bound (left) assumes independence and the upper bound (right) assumes perfectly correlated bar failures. Since limit state functions for failure of individual bars depend on the same set of random variables, bar failures are likely to be correlated. Hence, the upper bound ($P[\text{module failure}] \leq 1.70 \times 10^{-9}$) is probably more appropriate.

5.4.2 Failure of the suspension chain

The modules of the suspension chain are connected as a series system, i.e., failure of any of the modules leads to failure of the suspension chain. Each suspension chain is composed of 46 modules, with 11 modules belonging to the central truss. Disconsidering central truss modules, that makes 35 modules in a chain, and 70 modules for 2 chains. Assuming perfect correlation between module failures, failure probability of the suspension chain is equal to the failure probability of one module. Assuming independence between module failures leads to:

$$\begin{aligned} P[\text{chain failure}] &= 1 - \prod_{i=1}^{35}(1 - P[\text{failure module } i]) \\ &= 1 - (1 - 1.70 \times 10^{-9})^{70} = 1.19 \times 10^{-7} \end{aligned}$$

Hence, unimodal failure bounds for chain failure, assuming independence (left) and perfect correlation (right) are:

$$1.70 \times 10^{-9} \leq P[\text{chain failure}] \leq 1.19 \times 10^{-7}$$

Once more, assuming positive correlation between module failures seems more reasonable, hence the suspension chain failure probability is more likely to be closer to the upper bound (right).

6 Conclusion

The paper has shown how numerical structural reliability analysis can be performed based on finite element models of a structure, by incorporating structural reliability algorithms with deterministic finite element codes. A structural reliability module was developed and linked to the ANSYS finite element program.

The developed module provides an efficient and accurate scheme for solving structural reliability problems. It begins by searching design points, and makes intelligent use of design point location. Construction of response surfaces around each design point reduces errors in failure probability estimation, and allows an accurate evaluation of multi mode failure probabilities through importance sampling. If the numerical finite element model is not too large, importance sampling simulation can be performed directly on the finite element model, avoiding errors introduced by curve fitting.

Structural reliability analysis using the developed module becomes quite simple, requiring small additional effort in comparison to a traditional deterministic analysis. The feasibility of a numerical structural reliability analysis has been demonstrated through the solution of some example problems. These included non-linear and large scale structural problems.

The study of two very simple problems has shown the highly non-linear relation between safety coefficients and failure probabilities. It reveals the weak role of *safety* coefficients as determinators of structural safety.

Future research includes the incorporation of time-variant structural reliability methods and random vibration analysis of structures under the action of time-varying loads.

Acknowledgments: The financial support of this research by the Brazilian Councils for Research and Development (CNPq) and for Development of Higher Education (CAPES) is greatly appreciated.

References

[1] A. H-S. Ang and W. H. Tang. *Probability Concepts in Engineering Planning and Design.* John Wiley & Sons, 1990. Volume II: Decision, Risk and Reliability.

[2] *ANSYS User's Manual for Revision 5.0.* December 1992. Volumes I e II - Procedures.

[3] A. T. Beck. A reliability method for finite elements. Master's thesis, Universidade Federal de Santa Catarina (in portuguese), 1999. Pós-graduação em Engenharia Mecânica.

[4] A. T. Beck and E. da Rosa. *ACE-Pro - A Manual for Using and Programming*. GRANTE - Grupo de Análise e Projeto Mecânico, Pós-graduação em Engenharia Mecânica, Universidade Federal de Santa Catarina, 1999. (in portuguese).

[5] U. Borgund and C. G. Bucher. *Importance Sampling Procedure Using Design Point - ISPUD - User's Manual*. Institute für Mechanik, Universität Innsbruck, Innsbruck, 1986.

[6] K. Breitung. Asymptotic approximations for multinormal integrals. *Journal of Engineering Mechanics, ASCE*, 110(3):357–366, 1984.

[7] D. Ditlevsen. Principle of normal tail aproximation. *Journal of the Engineering Mechanics Division, ASCE*, 107(EM6):1191–1208, 1981.

[8] A. D. Kiureghian, M. Asce, and P-L Liu. Structural reliability under incomplete probability information. *Journal of Engineering Mechanics*, 1:85–103, 1986.

[9] P-L Liu and A. D. Kiureghian. Finite element reliability methods for geometrically nonlinear stochastic structures. Technical report, Department of Civil Engineering, University of California, Berkeley, 1989. report no. UCB/SEMM-89/05.

[10] P-L Liu and A. D. Kiureghian. Finite element reliability of geometrically nonlinear uncertain structures. *Journal of Engineering Mechanics*, 117(8):1806–1825, 1997.

[11] G. Maymon. Probability of failure of structures whitout a closed form failure function. *Computers & Structures*, 49(2):301–303, 1993.

[12] R.E. Melchers. *Structural Reliability Analysis and Prediction, second edition*. John Wiley and Sons, NY, 1999.

[13] E. Nikolaidis, D. Ghiocel, and S. Singhal. *Engineering Design Reliability Handbook*. CRC Press, 2005.

[14] R. Rackwitz and B. Fiessler. *Structural Reliability Under Combined Load Sequences*, volume 9. Computers and Structures, 1978.

[15] G. I. Schuëller and R. Stix. A critical apraisal on methods to determine structural reliability. *Structural Safety*, 4:293–309, 1987.